Physics and Chemistry of the Earth, special issue for the first European radar meteorology conference (ERAD) in Bologna, Italy, 4-8 September 2000.

Clear-air scattering observations: downdraft and angels

Victor Venema, Herman Russchenberg, Leo Ligthart

IRCTR, International Research Centre for Telecommunications-transmission and radar,
Department of Information Technology and Systems, Delft University of Technology, The Netherlands.

Abstract. This paper discusses two observations: a dual-frequency measurement of a downdraft and a high temporal measurement of a dot angel. The downdraft was measured with both an S-band (9-cm) and an X-band (3-cm) radar; it was observed to fall from 3-km height through a mist layer to the ground level. In the mist layer (in the lowest 1.2-km of the atmosphere) the difference in radar reflectivity factor was 3 dB, which is close to the expected 0 dB; in the downdraft it was about 23 dB; close to the 19 dB expected by the theory on coherent scatter. This demonstrates that it is possible to observe downdrafts by means of dual-frequency radar systems.

In measurements where the S-band Delft Atmospheric Research Radar (DARR) pointed vertically dot angels were observed. These dot angels are also referred to as worms, or ghosts, and it is speculated that they originate from the reflections of insects, birds, leaves, atmospheric plankton (anything organic in the air) or spontaneous turbulence. These dot angels are observed with an unprecedented high temporal resolution of 5 milliseconds using raw radar data. In this data we found that the dot angel had an interference pattern. Furthermore, the unwrapped phase indicates a point scatterer which follows a circular trajectory.

1 Introduction

This article treats two clear-air phenomena: a downdraft and a dot angel. The two phenomena may be related. The dot angel is a point target. The morphology of the radar reflectivity of the downdraft indicates that it may be composed of relatively few targets, so the downdraft may be composed of dot angels.

The downdraft has been measured using a dual-wavelength radar setup with an S-band and an X-band radar. This measurement method has recently been used to measure young cumulus clouds (Knight and Miller, 1998; Baker et al., 1998), a smoke plume (Rogers and Brown, 1997), and to distinguish between Rayleigh and Bragg scattering in the troposphere (Gage et al., 1999).

The dot angel has been measured by an S-band radar at a very high temporal resolution of 5 ms. These dot angels are sometimes referred to as worms, or ghosts. Speculations on the origin range from insects or birds to leaves, atmospheric plankton (anything organic in the air) or spontaneous turbulence. The angels reported in literature may have multiple origins. Ottersten (1970) has made an interesting and detailed year-long study of the atmospheric conditions un-

Correspondence to: Victor Venema, Victorv@dds.nl, fax: +31-15-2784046, http://irctr.et.tudelft.nl/~venema/

Table 1. Specification of the Delft Atmospheric Research Radar; between square brackets are typical values.

DARR specifications	
Radar type	FM-CW; linear modulation
Transmitted power	90 W
Transmitter	Solid state amplifier
Receiver noise figure	1 dB
Frequency	3.315 GHz
Wavelength	9.04 cm
Frequency excursion	1-50 MHz [5 or 10 MHz]
Sweep time	0.625-640 ms [1.25 or 2.5 ms]
Maximum range	0.5-30 km [4 or 8 km]
Range resolution	typically 15 or 30 m
Temporal resolution	5.12 s (averaging time 2.56 s)
Sampling frequency	100 kHz
Antenna gain	32.7 dB receiver
	40.0 dB transmitter
Antenna beam width	3.0° receiver
(Full-Width Half Power)	1.5° transmitter
	1.8° effective
Antenna diameter	4.28 m transmitter
	2.12 m receiver
Antenna isolation	> 90 dB

Table 2. Specification of SOLIDAR; between square brackets are typical values.

SOLIDAR specifications	
Radar type	FM-CW; linear modulation
Transmitted power	1 W
Transmitter	Solid state amplifier
Receiver noise figure	2.5 dB
Frequency	9.47 GHz
Wavelength	3.17 cm
Range resolution	typically 15 or 30 m
Temporal resolution	5.12 s (averaging time 2.56 s)
Sampling frequency	100 kHz
Antenna gain	38 dB
Antenna beam width	1.7° (Full-Width Half Power)
Antenna diameter	1.1 m
Antenna isolation	> 60 dB

der which (dot and layer) angels occur using S-band radar data. He concludes that dot angels are mainly caused by insects and birds.

2 Specifications of the radars

In this study two radars are used. The first radar is the Delft Atmospheric Research Radar, DARR: an S-band system (wavelength of 9 cm) equipped with parabolic antennas. The specifications of DARR can be found in Table 1. The antenna systems can be pointed in any direction, but during the measurements presented in this paper it always pointed towards the zenith.

The second radar is SOLIDAR: an X-band system (wavelength 3 cm), see Table 2 for the specifications. In the past this system was used in a scanning mode for detailed rain research (Ligthart and Nieuwkerk, 1990). For the measurements in this paper the antennas pointed to the zenith. Both radars use the same real-time data processing; the sweep time, frequency excursion and thus maximum range are the same in these measurements for both systems. This new setup has not yet been carefully calibrated and optimised. The conditions for combined measurements are ideal as the beam width of both antenna systems is about the same, as are the range and time resolution of both radars, and the radars are located close together.

Both radars operate according the Frequency Modulated Continuous Wave (FM-CW) principle (Russchenberg, 1992; Ligthart and Sinttruyen, 1992; and Skolnik, 1981).

The velocity measurements use the phase change that is associated with the movement of the target between two

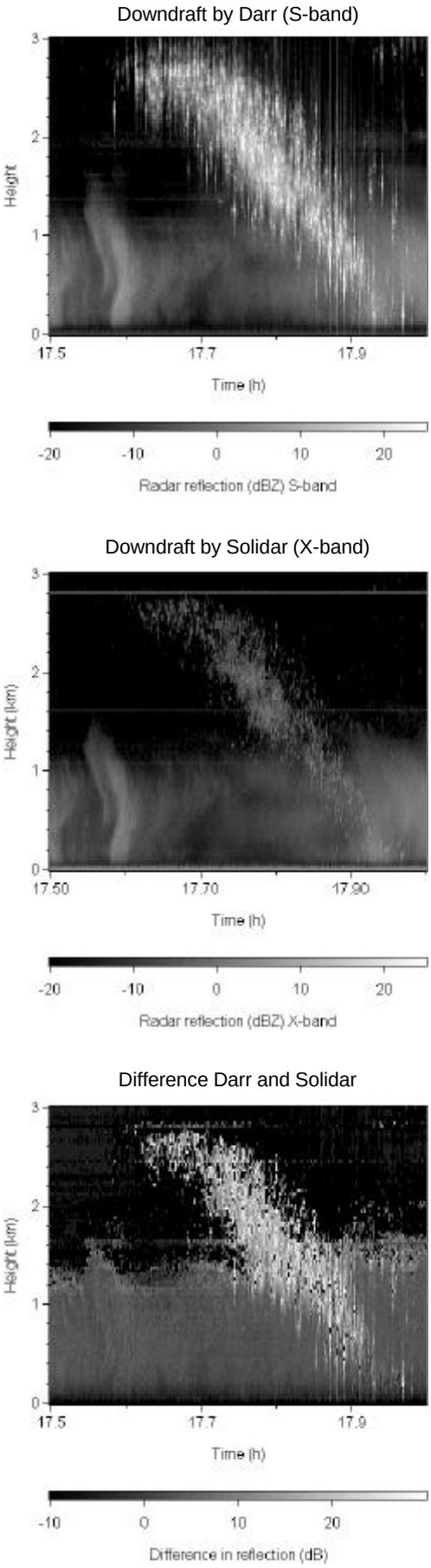

Figure 1. Downdraft (high reflections in the middle) in the mist (below 1 km) measured with the S-band radar DARR (9 cm) and the X-band radar SOLIDAR (3 cm) on the 23rd of February 1998. Both instruments pointed to the zenith.

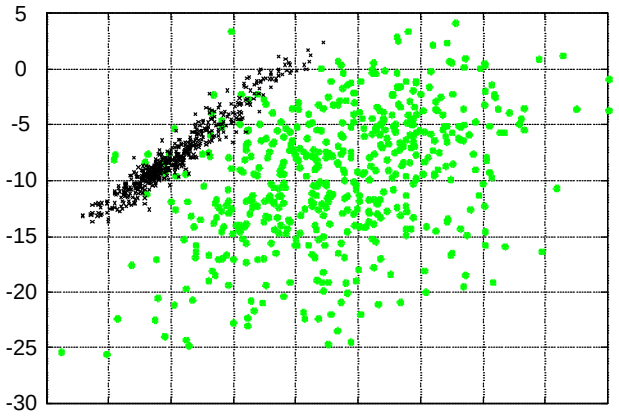

Figure 2. Scatter plot of the radar reflectivity factors at X and S-band for part of the mist and downdraft measurement. The crosses are data points taken in the mist and the grey dots are data points taken in the downdraft. The lines represent an equal radar reflectivity factor (pure incoherent Rayleigh scattering) and a 19 dB stronger reflections at S-band (pure coherent scattering with -5/3 slope).

measurements in a specific range cell. The difference in the two-way path between the radar and a target moving with constant speed (v) for time Δt is $2v\Delta t$. The phase change that corresponds to this is:

$$f_D(t) = 2p\frac{2v\Delta t}{l} \tag{1}$$

with ϕ_D the phase difference in [rad] between two sweeps, λ the wavelength, and Δt the time difference between two sweeps.

The phase of the signal cannot only be used to determine the velocity, but also the *relative* position of a single point source in a range cell compared to a reference position taken at a specified time. A limitation of this method is that the movement between two measurements (Δt) should not exceed $\lambda/4$, otherwise a reliable correction for 2π-jumps in the phase is impossible as the phase can only be measured within an interval of $(-\pi, \pi]$.

The power received by the radar (P_r) can be related to the properties of a single radar target if we take into account the system constants using the radar equation (Skolnik, 1981):

$$P_r = \frac{P_t G_t G_r l^2}{(4p)^3 r_d^4} s \tag{2}$$

with P_t the transmitted power in [W], G_t and G_r the gain of the transmitting and receiving antenna, λ the wavelength in [m], r_d the distance between the radar and the target (the range) in [m], σ the radar cross section of the target in [m^2]. Equation (2) is for a single target, e.g. a bird, insect or plane The backscattered power of a point target is inversely proportional to the 4th power of the range, as we assume that both the transmitted and the reflected wave expand isotropically.

The radar equation for volume scatterers is given by (Russchenberg, 1992):

$$P_r = \frac{P_t G_t G_r q_b^2 p^3 |K|^2 \Delta r}{512(\ln 2) l^2 r_d^2} Z \tag{3}$$

with θ_b the -3dB full beam width in [rad], $|K|^2$ = 0.93, a constant that accounts for the refractive index of the object and Z the equivalent radar reflectivity factor. Equation (3) applies to a volume with targets, e.g. a cloud, rain, a volume with spatial refractive index variations, or a group of insects. The radar equation for volume scatterers, Eq. (3), is inversely proportional to the square of the range because the volume of the radar range cell (and thus the number of targets) increases with the square of the range.

The calibration constants of both radars are determined by calibrating the separate system components like the output power, the antenna patterns, etc. With this method the accuracy of the calibration is about 1 dB.

A radar can receive reflections from spatial variations in the radio refractive index of the air, which we call here coherent air scattering. The pressure, temperature and humidity of the air determine the radio refractive index of the air. In the troposphere, this kind of scattering is mainly caused by spatial variations in humidity and temperature (Gossard and Strauch, 1983). The strength of the radar reflectivity per unit volume is given by (Ottersten, 1969):

$$h = 0.38 C_n^2 l^{-1/3} \tag{4}$$

where C_n^2 is a measure of the total variance of the spatial refractive index variations. An assumption in Eq. (4) is that the refractive index variations are in the inertial subrange and that the slope of the turbulent variance spectrum (-p) is -5/3. This type of scatter depends much less on the wavelength of the radar than that of incoherent scatter by particles. This means that coherent air scatter is more important when radars with a long wavelength are used.

3 Downdraft

The downdraft measurement shown in Fig. 1 is a good example of the ability of dual-wavelength radars to distinguish between coherent and incoherent scatter, see also the findings of Gage et al. (1999). Figure 1a is the reflection of DARR (wavelength of 9-cm). In the lower 1.2 km of Fig. 1 there is some drizzle or mist (velocities from 1.5 to 3.0 m/s downward). In the middle, from 3 km to the ground, one can see a downdraft, giving strong reflections with a speckled pattern (velocities in the top part range from 0.6 to 1.2 m/s downward). Such a downdraft measurement is very rare, but we have measured the phenomenon itself more

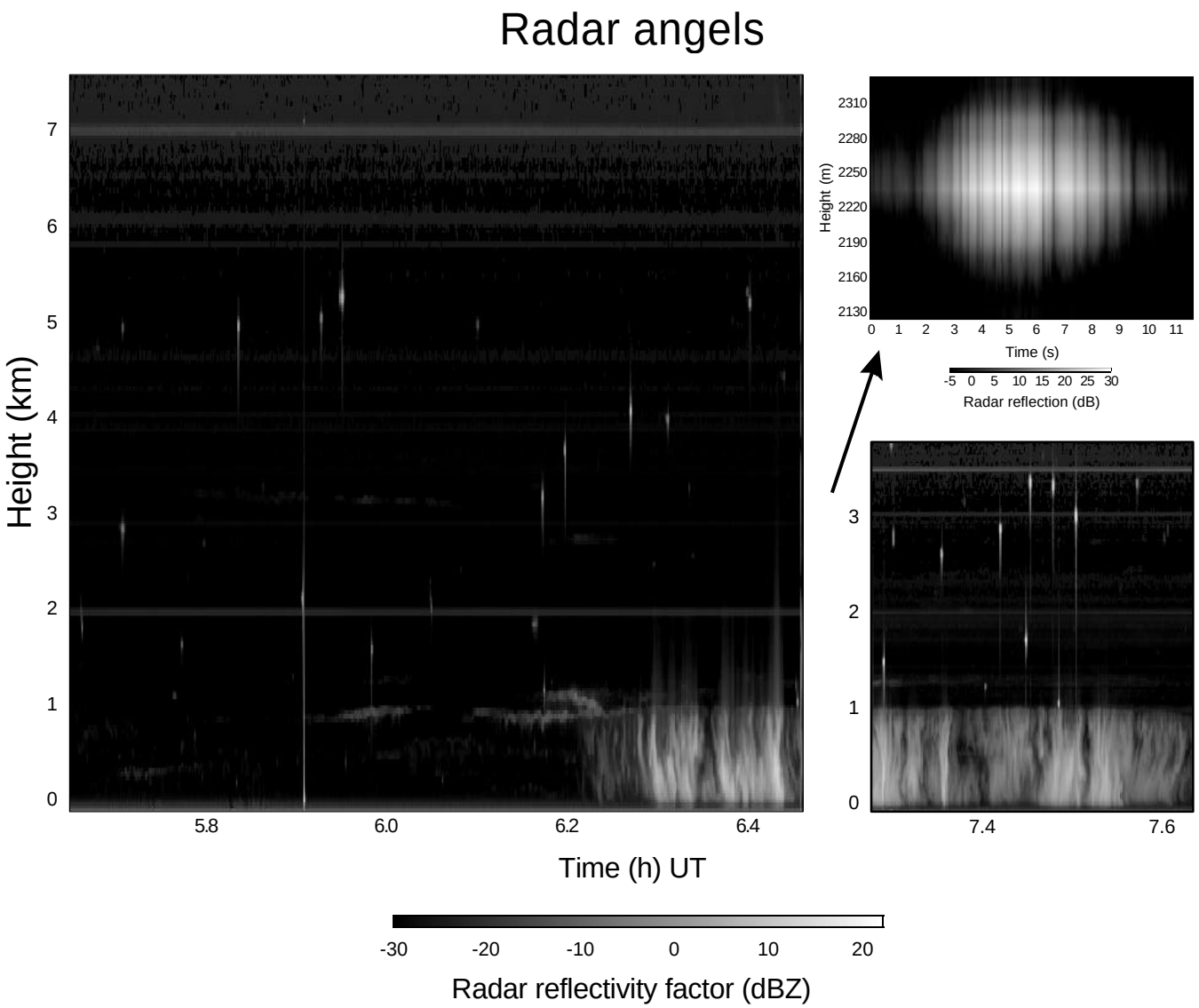

Figure 3. Measurement of Angels performed with DARR on the 4th of September 1996. The picture at the left and bottom right show the radar reflectivity factor calculated using the standard processing with a temporal resolution of 5.12 s. The high temporal image (top right) has a resolution of 5 ms. To get local summer time add two hours.

often. Figure 1b shows the same event with SOLIDAR (3-cm). Figure 1c shows the difference in radar reflection between the two radars.

The type of scattering can be distinguished by using the difference in radar reflectivity between the S- and the X-band radar (DZS–X), see Figure 2. Radar reflections from small Rayleigh particles (expressed in dBZ) should be the same for the two radars and reflections from coherent air scattering should give a difference of about 19 dBZ.

The DZS–X in the mist layer is not the expected 0 dBZ, but about 3 dBZ. A similar difference is reported by Bellon et al. (1997). They explain the difference in radar reflectivity between an UHF-profiler (32.8 cm) and an X-band radar by attenuation due to the radome. However, soaking the radome of SOLIDAR did not increase the DZS–X during a measurement of very light rain. Before this experiment the radome of SOLIDAR, made of bizonyl, had been renewed. The radome attenuation hypothesis therefore requires more attention. Inaccuracies or errors in the calibration and processing cannot be excluded as the setup is still new, but in this case the error should be larger than expected. A speculative explanation is that the radar reflectivity factor at S-band is enhanced due to coherent particle scattering by spatial structures in the rain. In this case, however, the scattering due to the structures would have to be much larger than expected from the coherent particle scattering theory of Erkelens et al. (2000).

The DZS–X of the downdraft is 23 dBZ. For coherent air scatter by fully developed isotropic homogeneous turbulence one would expect 19 dBZ difference in radar reflectivity. The fact that this difference is too large as well is an argument in favour of the explanation that the deviation from theory is due to a calibration error or due to attenuation by the wet radome.

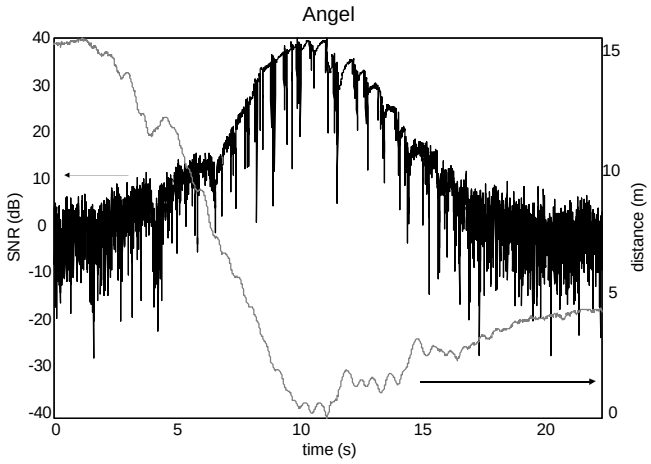

Figure 4. Measurement of an Angel with DARR. This line graph is made from a cross section of the Angel in Fig. 2 at 2235 m. The highly fluctuating line is the signal-to-noise ratio of the Angel. The smooth grey line is the unwrapped phase of the Angel converted into a measure of the relative distance to the radar.

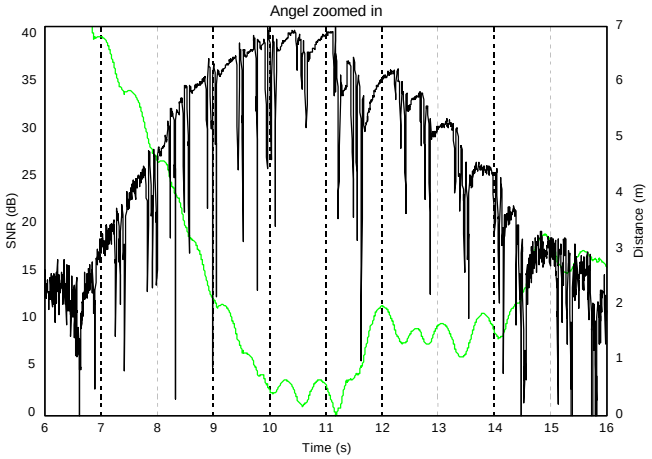

Figure 5. Zoom of the Angel in Fig. 3. The highly fluctuating line is the signal-to-noise ratio of the Angel. The smooth grey line is the unwrapped phase of the Angel converted into a measure of the relative distance to the radar.

The scatter in the DZS–X is very large. This is due to the speckle and the cross-talk in the range which can be seen in Fig. 1. Apparently there are just a few scattering sources in every radar cell. This is surprising as one would expect a volume with spatial refractive index variations caused by homogeneous turbulence to have many scattering centres. There are, unfortunately, no general theories on scattering by turbulence that is not fully developed, so a complete explanation for these measurements may not be possible.

4 Angel

Radar sometimes observes strong point reflections and layered reflections the origin of which is still unknown. These are called angels, worms, or ghosts, and it is speculated that these reflections originate from insects or birds (Glover et al., 1966), leaves, atmospheric plankton (anything organic in the air) or spontaneous turbulence (Ottersten, 1970).

The dot angels observed by Ottersten (1970) mainly occurred from May to September and the maximum activity was between 600 and 900 m. The dot angels are mainly seen during the day; the main activity starts when the ground has warmed up. At night Ottersten also observed dot angels, but these were much larger than the daytime type. The signals from the dot angels were symmetrical (in time) and either smooth, erratic or with a beat pattern having periods of a few Hz up to a few tens of Hz.

Angels are seen by an FM-CW system as small dots or vertical stripes due to cross talk in the Fourier transform. Examples of this type of angel are shown in Figure 3. The two overview measurements, which were made with the standard processing with a 5-second temporal resolution, show a light-rain event in the morning with angels above it; they are seen up to 5 km height. In between these two measurements, the beat signal of the radar was stored. This detailed measurement (top right) has a time resolution of 5 ms, which is the time between the sweeps of our FM-CW radar (one sweep is comparable to one pulse of a pulse radar). The measured thickness of the object is due to the signal processing (crosstalk in range). This high temporal resolution provides new insight into these angels. An interference pattern in the power is seen and a sinus pattern in the phase.

The pattern in the reflected power (signal-to-noise ratio, SNR) is more obvious in the line graphs of Figures 4 and 5. Both line graphs are taken from the range cell at a height of 2235 m. The maximum SNR (= 40 dB) corresponds with a radar cross section of 1.1 cm^{-2} in case the dot angel drifted exactly overhead the radar antenna beam. In case it went through the beam a little bit off the middle, the radar cross section will be larger. Part of the power from the range cell at 2235 m has leaked to other range cells due to crosstalk, therefore the real radar cross section will be larger as well.

Insects have a radar cross section of 0.01 to 1 cm^{-2}, a sparrow has one of 14 cm^{-2} and a pigeon one of 80 cm^{-2} (Skolnik, 1981). The full -3 dB beam width at the height of the angel is about 70 m. The -3 dB width of the angel in Fig. 5 is about 3 sec, so if we assume that the bird scatters isotropically and flies over the middle of the antenna it has a flying speed of about 20 m/s. Birds fly typically with a speed of 8 to 20 m/s (Skolnik, 1981). If the general shape of the SNR is due to an angular dependence of the radar cross section, the speed can be much lower. The wind speed (from a radiosonde) at this height is about 5 m/s, the temperature 6 °C and the humidity 46 percent.

The figures above also show the unwrapped phase (distance) of the measured signal, which has a sinus pattern. The measured phase was unwrapped, i.e. corrected for 2π jumps by a simple algorithm that compared two consecutive phases and added or subtracted 2π if that would reduce

the phase difference. The scattering object is probably a point target. In this case the phase can be converted into a distance (with an arbitrary starting point). A part of the general trend in the phase can be explained by the phase pattern of the antenna and a part of this may be explained by a change of distance associated with a horizontal movement of the dot angel through the beam.

Fig. 5 shows that at the moments that the SNR is irregular, the unwrapped phase is at a minimum (after the trend has been removed). Furthermore, it shows that the tops of the sinus patterns in the phase correspond to the periods in which the SNR is smoothly increasing. The period of the unwrapped phase signal is about 0.8 seconds. And after the trend has been removed, the maximum amplitude of the unwrapped phase is 0.5 m. A second angel found in the beat signal of the radar showed similar interference patterns in the SNR, but the quality of this measurement was not good enough so we could not unwrap the phase.

5 Conclusions

We could identify a downdraft as a coherent scattering phenomenon using dual-wavelength radar measurements. The difference in radar reflectivity factor between S-band and X-band in the mist and in the downdraft is larger than the theoretically expected values. The cause of this difference should be investigated. An upgrade of both radar systems is planned. After this upgrade both systems will be able to measure the same maximum velocity and the sensitivity of SOLIDAR will be increased, which will allow even better comparisons between the systems. After this upgrade the calibration should be carefully checked. Furthermore, the upgrade will make it possible to investigate the influence of a wet radome on radar measurements when it does not rain.

The radar cross section of dot angels corresponds to that of birds, as does the speed at which the angels move through the antenna beam. However, we still need to investigate whether birds (or bird's wings) can produce the fascinating interference patterns seen in the SNR and in the sinus pattern in the unwrapped phase.

Reference

Baker, B., J. Brenguier, and W. Cooper. Unknown Source of Reflectivity from Small Cumulus Clouds. *Cloud Physics Conf.*, Everett, Washington, 1998.

Bellon, A., I. Zadwadzki, F. Fabry. Measurements of melting layer attenuation at X-band frequencies. *Radio Sci.*, **32**, no. 3, pp. 943-955, 1997.

Erkelens, J.S., V.K.C. Venema, H.W.J. Russchenberg, and L.P. Ligthart. Coherent scattering of microwaves by particles; Evidence from clouds and smoke. *J. Atmos. Sci.*, Accepted, 2000.

Gage, K.S., C.R. Williams, W.L. Ecklund, and P.E. Johnston. Use of Two Profilers during MCTEX for Unambiguous Identification of Bragg Scattering and Rayleigh Scattering. *J. Atmos. Sci.*, **56**, pp. 3679-3691, 1999.

Glover, K.M., K.R. Hardy, T.G. Konrad, W.N. Sulivan, and A.S. Michaels. *Science*, **154**, pp. 967, 1966.

Gossard, E.E., and R.G. Strauch. *Radar Observations of Clear Air and Clouds*. Elsevier, 280 p., 1983.

Knight, C.A., and L.J. Miller. Early radar echoes from small, warm cumulus: Bragg and hydrometeor scattering. *J. Atmos. Sci*., **55**, pp. 2974-2992, 1998.

Ligthart, L.P., and L.R. Nieuwkerk. An X-band solid-state FM-CW weather radar. *IEE Proc. F. Comm. Radar & Signal Process.*, **137**, no. 6, pp. 418-426, Dec. 19990.

Ligthart, L.P., and J.S. van Sinttruyen. FM-CW radar polarimetry. *Direct and inverse methods in radar polarimetry, part 2*, W.-M Bourner et al. (eds.), pp. 1625-1657, 1992.

Ottersten, H. *Radar angels and their relationship to meteorological factors.* FOA reports, **4**, no. 2, 33 p., Forvarets Forskningsanstalt, Stockholm, Sweden, 1970.

Ottersten, H. Radar backscattering from the turbulent clear atmosphere. *Radio Sci.*, **4**, pp. 1251-1255, 1969.

Rogers, R.R, and W.O.J. Brown. Interactions Between Scattering by Precipitation and the Clear Air. *Proc. 8th URSI Comm. F triennial Open Sym.*, pp. 235-238, 22-25 September, 1998.

Rogers, R.R., and W.O.J. Brown. Radar observations of a major industrial fire. *Bull. Amer. Meteor. Soc.*, **78**, pp. 803-814, 1997.

Russchenberg, H.W.J. *Ground-based remote sensing of precipitation using a multi-polarized FM-CW Doppler radar*. PhD dissertation, Delft University Press, Delft, The Netherlands, 206 p., ISBN: 90-6275-823-1, 1992.

Skolnik, M.I. *Introduction to radar systems; second edition.* McGraw-Hill, Singapore, 581 p., ISBN: 0-07-066572-9, 1981.